Polymer 50 (2009) 2601–2607

Contents lists available at ScienceDirect

Polymer

journal homepage: www.elsevier.com/locate/polymer

Stability and phase behavior of the poly(ethylene oxide)–urea complexes prepared by electrospinning

Yang Liu, Christian Pellerin*

Centre for Self-Assembled Chemical Structures (CSACS) and Département de chimie, Université de Montréal, Montréal, Québec H3C 3J7, Canada

ARTICLE INFO

Article history:
Received 8 January 2009
Received in revised form
16 March 2009
Accepted 18 March 2009
Available online 12 April 2009

Keywords:
Host–guest complex
Phase transitions
Electrospinning

ABSTRACT

The poly(ethylene oxide)–urea binary system forms a stable (α) complex that can be melt-quenched into a mixture of urea and a second (β) complex with a different stoichiometry. Our results confirm that this mixture is metastable, but that the β–α solid–solid transition is much slower than previously reported. In contrast with the melt-quenched mixture, we observe for the first time that the pure β complex, prepared by electrospinning, is thermodynamically stable up to its melting temperature. This melting is incongruent and leads to the formation of the crystalline α complex and liquid PEO. A phase diagram is drawn over the complete composition range and allows interpreting the formation of the various out-of-equilibrium mixtures observed experimentally. This work also demonstrates an interesting new possibility of electrospinning: the direct preparation of thermodynamically stable compounds that are otherwise inaccessible because of the formation of kinetically frozen products.

1. Introduction

The molecular complexes of poly(ethylene oxide) (PEO) and urea have received renewed attention in recent years. For instance, it was shown that they can form highly oriented fibers through electrospinning that could lead to new applications [1,2]. Nevertheless, a complete phase diagram has not yet been obtained for this binary system and the stability of the different complex forms is not fully established [3–6]. Up to now, three crystalline modifications have been reported for PEO–urea system. The stable α complex, with a $(EO)_4$–$(urea)_9$ stoichiometry, was first reported by Tadokoro et al. [3]. Brisse and Chenite prepared single crystals and showed that it belongs to the trigonal system with $a = b = 1.054$ nm, $c = 0.912$ nm, and $\gamma = 120°$ at 173 K [4]. A different crystalline structure was reported for the complex of urea with low molecular weight PEO ($M_w = 400$ Da), with a 1:1 PEO:urea molar ratio and a tetragonal unit cell ($a = b = 0.73$ nm, $c = 1.951$ nm) [7]. Finally, Bogdanov et al. prepared a third crystalline PEO–urea complex (called "melt-quenched" β hereon) by quenching the α complex from above its melting temperature [8–11]. It has been hypothesized [5] that it could adopt the hexagonal structure ($a = b = 0.819$ nm, $c = 1.103$ nm) observed for the urea complexes with other polymers [12–14] and small molecules [15], or that it adopts the tetragonal structure of the low molecular weight PEO–urea complex [16].

The observation of two stoichiometric complexes has also been reported by Damman et al. for PEO with other host molecules, such as resorcinol [17] and p-nitrophenol [18–20]. In both cases, the β form was found to be metastable and to rapidly transform into the stable α form [21]. In contrast, two thermodynamically stable complexes were observed for the PEO system with 2-methyl resorcinol (MRES) [22,23]. The low-melting point complex (7:2 PEO:MRES molar ratio) possesses a layered structure, while the 3:1 complex forms a tight hydrogen-bonded network and shows a higher melting temperature. It is well known that the melt-quenched PEO–urea β samples can rapidly convert back to the α form when heated above 90 °C [8–11]. Importantly, Ye et al. have recently showed that a solid–solid β–α transition can take place slowly at much lower temperatures, even at room temperature, suggesting that the complex is in fact metastable [16].

A limiting factor in the study of the PEO–urea system has always been the preparation of pure samples of the β complex. In spite of efforts to isolate it, wide-angle X-ray diffraction (WAXD) patterns of the melt-quenched sample usually reveal the presence of some residual urea or α complex. This experimental difficulty has left open the question of whether the β complex is stable or metastable by itself, therefore preventing the drawing of a complete phase diagram and a proper understanding of the complex phase behavior.

* Corresponding author. Centre for Self-Assembled Chemical Structures (CSACS) and Département de chimie, Université de Montréal, CP 6128 Succ. Centre-ville, Montréal, Québec H3C 3J7, Canada. Tel.: +1 514 340 5762; fax: +1 514 340 5290.
E-mail address: c.pellerin@umontreal.ca (C. Pellerin).

0032-3861/$ – see front matter © 2009 Elsevier Ltd. All rights reserved.
doi:10.1016/j.polymer.2009.03.050

In a recent paper, we have shown that it is possible to prepare almost pure samples of both α and β complexes in bulk amounts using electrospinning [2]. In this technique, a large electric field is applied to an entangled polymer solution to produce nanofibers [24–26]. It has been shown that electrospinning can impart molecular orientation parallel to the fiber axis [1,27,28] and that it sometimes produces metastable structures [29,30]. In our previous work, the α and β complex fibers presented a high level of crystallinity and orientation without the need for a thermal annealing or mechanical deformation [2]. WAXD and Fourier transform infrared (FT-IR) spectroscopy characterization of these electrospun fibers revealed that the stoichiometry of the pure β complex is $(EO)_3$–$(urea)_2$, and suggested a layered orthorhombic crystal structure with a = 1.907 nm, b = 0.862 nm and c = 0.773 nm [2]. This layered structure is reminiscent of that of the stable low-melting point complex of PEO with MRES [22]. The availability of these samples now allows revisiting the stability and phase diagram of the PEO–urea complexes. It will be shown using variable-temperature WAXD and FT-IR that the pure β complex is stable, in contrast with the melt-quenched sample. A phase diagram drawn using samples prepared by electrospinning will allow interpreting the rich phase behavior of the PEO–urea system.

2. Experimental section

2.1. Sample preparation

PEO with a weight-average molecular weight of 400 000 g/mol (Scientific Polymer Products) and, urea (Fisher Scientific) were used without further purification. The α complex was prepared using a previously described co-crystallization method [1]. The melt-quenched β sample was prepared by heating the α complex to 160 °C (17 °C above its melting point) and cooling it to room temperature at a rate of at least 10 °C/min. The pure β complex and the various samples used to determine the phase diagram were prepared by electrospinning solutions of PEO and urea in water. 0.5 g of PEO was dissolved in 10 ml of distilled water and an appropriate amount of urea was added to obtain mixtures with various PEO:urea molar ratios. A PEO:urea molar ratio of 3:2 was used to prepare samples of almost pure β complex. The solutions were introduced in a syringe equipped with a 0.41 mm diameter flat-end needle. A 15 kV positive voltage was applied on the needle tip using a CZE 1000R high-voltage power supply (Spellman High Voltage Electronics) while a 2 kV negative potential (Power Designs) was imposed on a rotating cylinder collector to collect the electrospun fibers. The as-prepared electrospun fibers were folded and ground to obtain randomly oriented samples for the following DSC, FT-IR and WAXD characterization.

2.2. Sample characterization

DSC measurements were conducted using TA Instruments 2910 or Q1000 calorimeters calibrated with ultra-pure indium. The heating rate was 10 °C/min and the cooling rate was either 10 or 3 °C/min. Infrared spectra with a resolution of 4 cm^{-1} were recorded on a Vertex 70 FT-IR spectrometer (Bruker Optics) equipped with a liquid nitrogen-cooled HgCdTe detector. Spectra were collected in the attenuated total reflection (ATR) mode using a MIRacle accessory (Pike Technologies) or a temperature-controlled GoldenGate accessory (Specac). Wide-angle X-ray diffraction measurements were carried out using a Bruker AXS diffractometer (Siemens Kristalloflex 780 generator), operated at 40 kV and 40 mA, using the Cu Kα (0.1542 nm) radiation collimated by a graphite monochromator and a 0.5 mm pinhole. The diffraction patterns were captured by a HI-STAR area detector. The samples were sealed in aluminum pans and their temperature was controlled by an STC 200 controller and an LN2-SYS liquid nitrogen cooling system (Instec). A scattering background was subtracted for display.

3. Results and discussion

3.1. Phase transitions of the α and melt-quenched complexes

Although the crystalline structure of the α complex has been established for many years, its phase behavior is still not fully understood. Fig. 1 shows the DSC thermograms of this complex during a heat–cool–heat cycle. During the first heating scan, the crystalline α complex melts at 143 °C, higher than the melting points of pure PEO (67 °C) and urea (135 °C). Two exothermic peaks appear during the cooling cycle at 10 °C/min, under conditions that produce the melt-quenched β complex. The first peak at 90 °C is very narrow and indicates a fast crystallization that is more typical of small molecules than polymers. The second exotherm at 65 °C, which has not been reported in the literature, is much broader, characteristic of the slower crystallization rate of polymers. The exothermic peak at 95 °C observed during the second heating ramp can be attributed to the β–α phase transition. The newly formed α complex melts at 140 °C and the melting enthalpy is 30% smaller than in the first heating scan, indicating a decreased level of crystallinity and less perfect crystals than in the original sample.

A firm attribution of these various thermal events is established by performing WAXD and FT-IR measurements during similar heat–cool–heat sequences [31,32]. Fig. 2 shows that the WAXD pattern of the original sample (top curve) only presents the characteristic peaks of the α complex, most notably the intense peak at 21.6° due to the 201 plane. Heating the sample to 160 °C melts the complex and only an amorphous halo is observed. Several crystalline reflections appear when temperature is decreased below 90 °C, with the most intense peak appearing at a 2θ angle of 22.2°. All these peaks can be indexed using the tetragonal unit cell of pure urea [33,34], confirming that the narrow exotherm at 90 °C in the cooling run of Fig. 1 is due to pure urea crystallization. This crystallization temperature is somewhat lower than for pure urea (101 °C) because the presence of PEO in the liquid phase increases the entropic cost of crystallization. The characteristic 410 reflection of the β complex appears at a 2θ angle of 21.2° when temperature

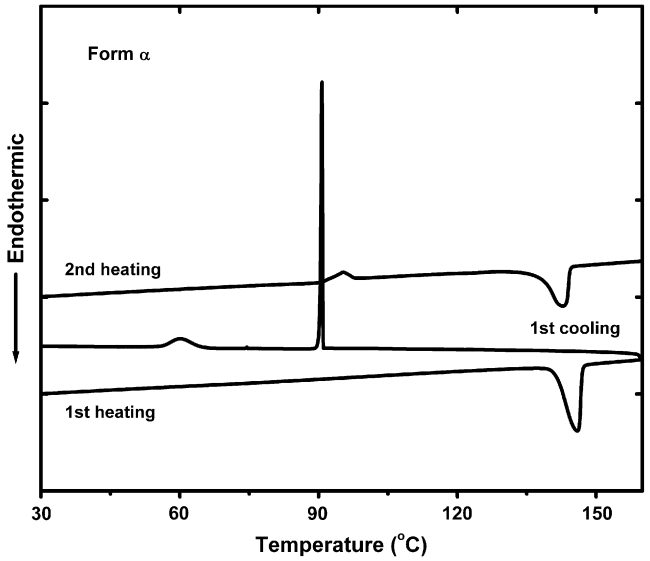

Fig. 1. DSC thermograms recorded for the PEO–urea α complex.

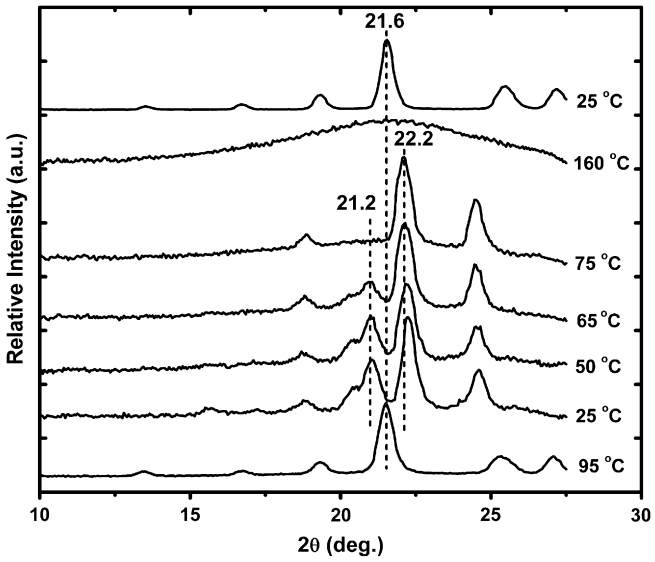

Fig. 2. WAXD patterns of the PEO–urea α complex recorded at 25 °C (top curve), after heating to the liquid state (160 °C), cooling to 75, 65, 50 and 25 °C, and finally after a second heating to 95 °C (bottom trace).

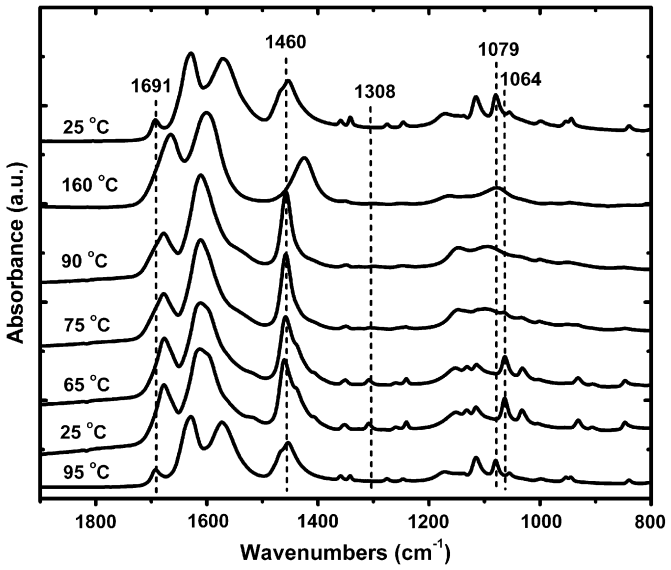

Fig. 3. FT-IR spectra of the PEO–urea α complex recorded at 25 °C (top curve), after heating to the liquid state (160 °C), cooling to 90, 75, 65 and 25 °C, and finally after a second heating to 95 °C (bottom trace).

reaches 65 °C and it becomes more prominent as temperature is further decreased. Meanwhile, the intensity of the pure urea peaks is maintained, proving that the melt-quenched sample is composed of a mixture of urea and the β complex. This is consistent with the stoichiometry of the two complexes, with PEO:urea molar ratios of 4:9 and 3:2 for the α and β complexes, respectively. Finally, the β complex and urea peaks disappear simultaneously and are replaced by those of the α complex when reheating the sample to 95 °C, confirming the β–α transition exotherm during the second heating cycle of Fig. 1. This phase transition occurs instantaneously on the time scale of WAXD at this temperature but the kinetics of the process at lower temperatures will be discussed below.

It is noteworthy that it is urea, and not the α complex, that partially crystallizes at 90 °C even if the latter has a higher melting point. This can be explained by a slower nucleation rate for the α complex due to the incorporation of PEO chains in the crystals. Polymers generally require a large degree of undercooling to crystallize at significant rates because of a slow nucleation process at temperatures close to their melting point. Urea crystals are therefore produced for kinetic and not for thermodynamic reasons. As a matter of fact, cooling the α complex melt at a slower rate of 3 °C/min only produces the thermodynamic product, the α complex crystals, and not a kinetically frozen mixture of urea and β complex.

The temperature-controlled FT-IR spectra shown in Fig. 3 confirm the WAXD results and provide additional molecular insight on this system. The spectrum of the initial α complex sample (top curve) is characterized by the presence of a urea amide band at 1691 cm^{-1} and by a PEO C–O–C stretching mode at 1079 cm^{-1}, as compared to 1098 cm^{-1} for pure PEO. The 1691 cm^{-1} band completely disappears and the C–O–C band becomes much broader upon melting the sample at 160 °C. When temperature is decreased to below 90 °C, the partial crystallization of urea is clearly observed through the blue shift of the C═O stretching and NH_2 deformation vibrations, and by the shift and narrowing of the C–N stretching band around 1460 cm^{-1}. Meanwhile, most PEO bands do not change with the exception of the C–O–C stretch that shifts to ~1090 cm^{-1}. This position indicates that the PEO chains are still hydrogen-bonded with urea in a melt with the β complex composition. These favorable enthalpic interactions decrease the Gibbs free energy of urea in the melt and explain the fact that urea only partially crystallizes during the DSC cooling scan. When temperature reaches 65 °C, the PEO bands become narrower and adopt the positions characteristic of the crystalline β complex, including a single CH_2 wagging band at 1351 cm^{-1}, a new band at 1308 cm^{-1}, and the C–O–C stretching band at 1064 cm^{-1} [2,16]. Shoulders on the urea bands around 1600 and 1518 cm^{-1} also indicate the coexistence of the solid β complex with pure crystalline urea [35]. The infrared spectra finally confirm β–α transition when temperature is increased above 95 °C.

3.2. Phase transitions of the pure β complex

The phase behavior of the pure β complex has never been studied in detail before. The first heating DSC thermogram of Fig. 4 shows two transitions at 89 and 143 °C. These temperatures are quite similar to those observed in the second heating cycle of Fig. 1 for the melt-quenched mixture. A noteworthy difference is that the

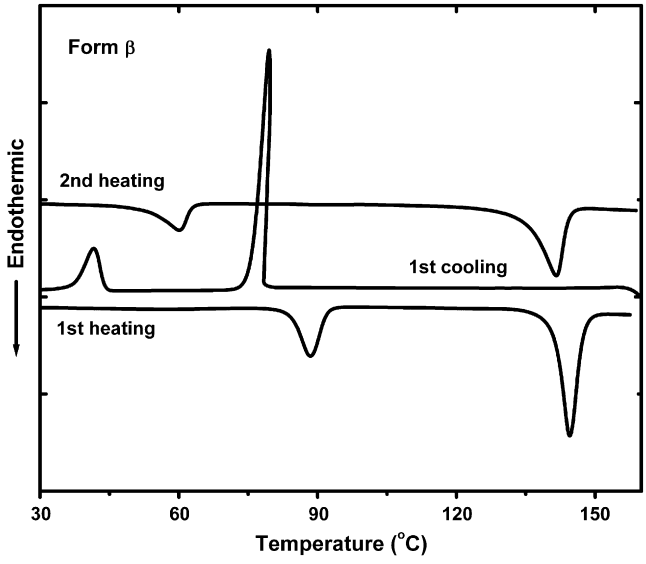

Fig. 4. DSC thermograms recorded for the pure PEO–urea β complex.

first thermal event is endothermic in Fig. 4 and not exothermic as in Fig. 1. We have previously shown using FT-IR spectroscopy that this peak is due to the conversion of the β complex into a mixture of the α complex and liquid PEO [2]. Assuming that the melting enthalpy of the α complex is 228 J/g (assuming in first approximation that the pure α complex is 100% crystalline), the 131 J/g melting enthalpy observed at 143 °C corresponds to a ~91% β–α conversion yield. Two exothermic peaks appear in the cooling run, as was observed in Fig. 1 for the α complex, but at temperatures ~15 °C lower. The exotherm at 75 °C is narrow, although not as much as for the urea crystallization in Fig. 1, while the peak at 40 °C is broad. Two endothermic peaks appear in the second heating ramp at 65 and 140 °C, close to the melting temperatures of pure PEO and of the α complex, respectively.

The temperature-controlled WAXD experiments of Fig. 5 were performed to confirm the nature of the coexisting phases. The original specimen at 25 °C only shows the characteristic reflections of the β complex, thereby confirming that electrospinning is a powerful method to prepare pure samples of this complex. When temperature is increased to 90 °C, all peaks disappear abruptly and are replaced by those of the α complex. A significant amorphous halo simultaneously develops, consistent with the presence of residual liquid PEO after the β–α conversion. After complete melting at 160 °C, the α complex diffraction peaks reappear directly when cooling to 75 °C at a rate of 10 °C/min. Crystallization of the α complex is slower than that of pure urea because of the involvement of the polymeric PEO chains, justifying the observation of a broader peak in Fig. 4 as compared to the urea crystallization in Fig. 1. Further cooling the sample below the broad exothermic transition at 40 °C provokes the crystallization of pure PEO, as confirmed by the characteristic 120 and 032 peaks of PEO at 19.0° and 23.2°, respectively. Degrees of crystallinity of ca. 70% and 61% are calculated for the α complex and for PEO assuming melting enthalpies of 228 and 182.7 J/g, respectively [36]. This is consistent with the weak amorphous halo observed in the WAXD pattern of Fig. 5 at the end of the cooling ramp. Finally, the second heating cycle sees the successive melting of the PEO and α complex crystals, as expected from Fig. 4. It is interesting to note that melt-cooling the α complex yields a mixture containing the β complex, while melt-cooling the β complex produces a mixture that contains the α complex. In order to explain this behavior, it is important to establish whether the pure β complex is stable or metastable.

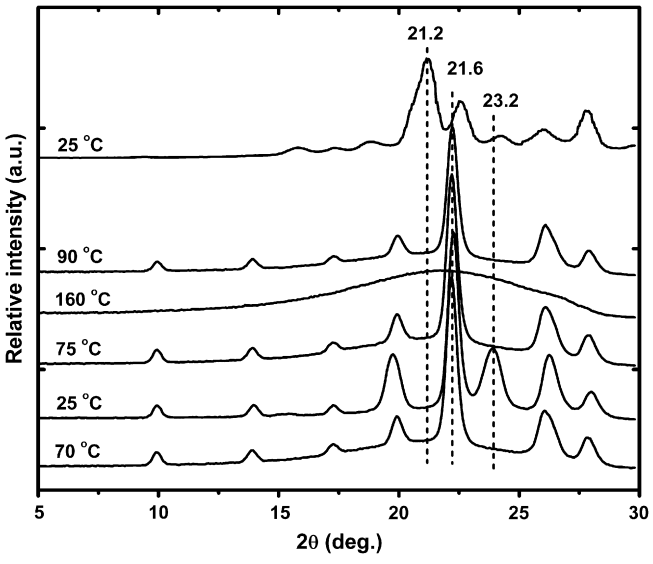

Fig. 5. WAXD patterns of the pure PEO–urea β complex recorded at 25 °C (top curve), after heating slightly above the phase transition temperature (90 °C) and in the melt state (160 °C), after cooling to 75 and 25 °C (middle curves), and finally after a second heating scan to 70 °C (bottom trace).

3.3. β–α Transition and stability of the pure β complex

It is now established that the melt-quenched β mixture can convert rapidly to the α form at 95 °C [8–11], as seen in Fig. 1, or more slowly at lower temperatures through a solid–solid transition [16]. Ye et al. have recently used infrared spectroscopy to follow the β–α transition kinetics during the annealing of melt-quenched samples and determined an activation energy of 222 kJ/mol for the process [16]. FT-IR spectroscopy and WAXD were employed here to obtain additional insight on this phenomenon. Fig. 6A confirms that the phase transition occurs quite rapidly at 60 °C, 35 °C below the DSC transition temperature. Indeed, all infrared bands of the β complex, including those at 1351 and 1308 cm^{-1} and the C–O–C stretch at 1064 cm^{-1}, disappear almost completely in less than 15 min and are replaced by bands of the α complex. The use of

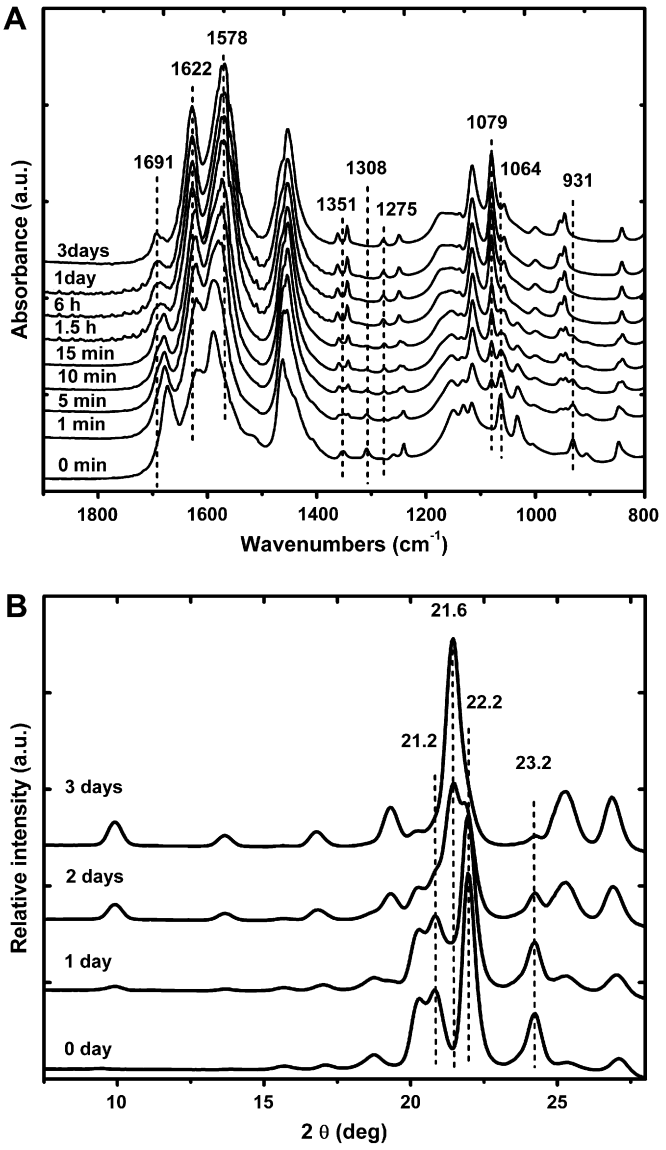

Fig. 6. (A) FT-IR spectra and (B) WAXD profiles of the melt-quenched β mixture recorded as a function of time during an annealing at 60 °C.

attenuated total reflectance (ATR) in this study allows following bands that were saturated in the transmission spectra of reference 16. As expected, the intense C═O and NH_2 modes at 1619 and 1589 cm^{-1} also shift to their final position in about 15 min. In sharp contrast, the 1675 cm^{-1} band continues blue shifting and only stabilizes at 1691 cm^{-1} after almost three days of annealing. Second derivative spectra show that this shift is actually due to the decrease of a β complex band at 1675 cm^{-1} coupled with the concomitant increase of an α complex band at 1691 cm^{-1}. Nevertheless, this result indicates that while the local scale conformational changes occur rapidly in a few minutes, the overall phase transition process is actually two orders of magnitude slower than previously thought.

This conclusion is confirmed by the WAXD measurements of Fig. 6B, in which the β complex and urea peaks at 21.2° and 22.2°, respectively, still largely dominate after one day of annealing at 60 °C. The α complex peak at 21.6° increases gradually and dominates the diffraction pattern after three days of annealing, with traces of β complex and urea left. The apparent position of 1691 cm^{-1} infrared band can therefore be used as an indicator of the large scale crystalline modifications as observed through X-ray diffraction. Similar behavior was observed at other temperatures, including at room temperature. In that case, the PEO infrared bands evolved from β to α over several hours, but the WAXD peaks only showed obvious α complex presence after weeks, taking several months to complete the solid–solid phase transition.

At first sight, it would appear that the pure β complex is also metastable since it features a similar β–α transition at 90–95 °C in the thermogram of Fig. 4. However, the infrared spectra of Fig. 7A show that the pure β complex remains unaffected by 24 hours of annealing at 60 °C. This is to be contrasted with Fig. 6A, in which the occurrence of the solid–solid phase transition was clear after less than 1 min for the melt-quenched sample. WAXD measurements (not shown) did not reveal any change either after more than a day of annealing, as was expected since the infrared spectra are much more sensitive to the local conformational changes occurring in initial stage of phase transition. Since the β–α DSC transition is lower for the pure β complex than for the melt-quenched sample (89 vs. 95 °C), one would rather have predicted a faster phase transition, assuming an equivalent activation energy. Fig. 7B shows the time evolution of the absorbance of the 1308 cm^{-1} band, which is well isolated and is characteristic of the β complex. It can be seen that, after 3 hours of annealing, the β–α transition is limited to 5% at 70 °C and 20% at 75 °C. A 24 hours annealing at 75 °C, the apparent onset temperature of the DSC transition peak, only amounted to the equivalent of approximately 1 min at 60 °C for the metastable melt-quenched sample. Pure β complex shows an almost complete formation of the α complex only when the annealing is performed at or above 80 °C, which corresponds to the maximum of the DSC endotherm at a scanning rate of 1 °C/min.

These results strongly suggest that the phase transition of the pure β complex is a thermodynamic process and not a kinetic transition, and that the metastability observed for the melt-quenched sample is due to the presence of residual urea. The partial transition occurring at 75 °C in Fig. 7B can be attributed to the incongruent melting of smaller or defective crystals, while larger crystals require a higher temperature to melt. The endothermic phase transition observed by DSC in Fig. 4 is therefore due to the overlap of the endothermic melting of the β crystals with the exothermic crystallization of the α complex. The pronounced temperature dependence of the transition kinetics observed in Fig. 7B further supports the thermodynamic stability of the pure β complex. If the β–α transition was a kinetic process, one would have expected it to possess a lower activation energy than the 222 kJ/mol determined for the melt-quenched sample [16]. Indeed, the latter requires disruption of urea crystals much below their melting temperature in order to form the channel structure of the α complex, while converting the pure β complex to the α complex only requires ejection of highly mobile PEO chains since they are well above their melting point of 67 °C.

3.4. Phase diagram of the PEO–urea system

Considering the newfound stability of the pure β complex, it is now possible to draw a complete phase diagram of the PEO–urea binary system. Fig. 8 is obtained by measuring the DSC thermograms of samples prepared by electrospinning solutions with various PEO:urea molar ratios. The nature of the different phases was confirmed by infrared spectroscopy and WAXD. The phase diagram contains two stable stoichiometric complexes at urea molar fractions (X_U) of 0.692 (α complex) and 0.4 (β complex). The α complex melts congruently at a higher temperature (143 °C) than the two starting components because of the strong hydrogen-

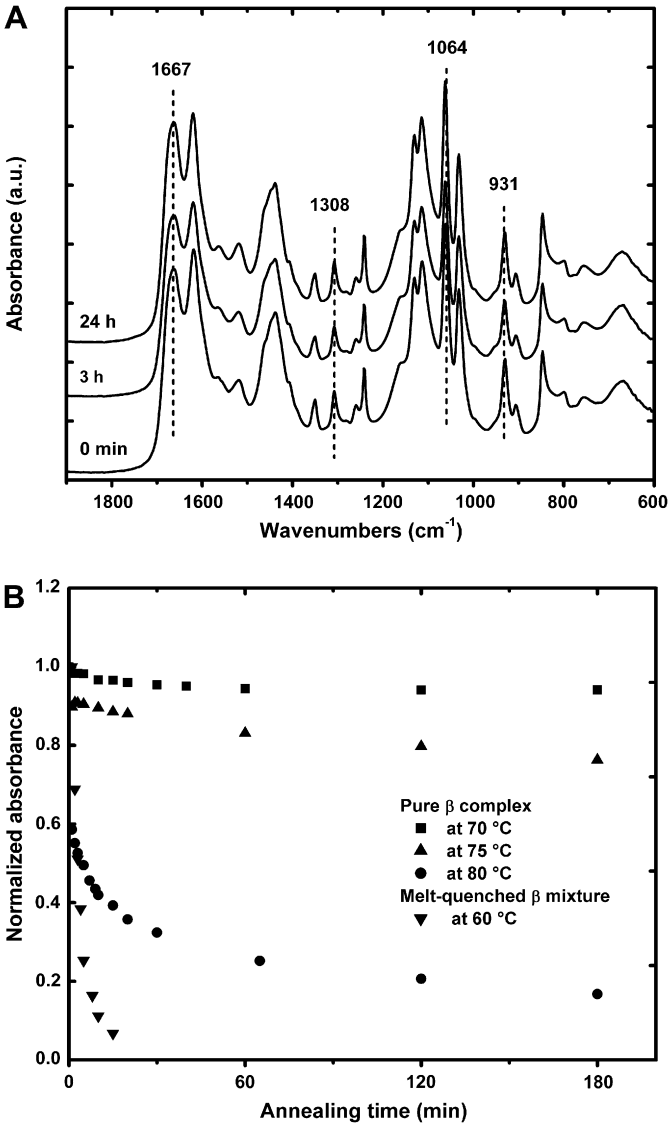

Fig. 7. (A) FT-IR spectra of the pure β complex recorded as a function of time during an annealing at 60 °C; (B) Time evolution of the normalized absorbance of the 1308 cm^{-1} β complex band during annealings at 70, 75 and 80 °C for the pure β complex and at 60 °C for the melt-quenched β mixture.

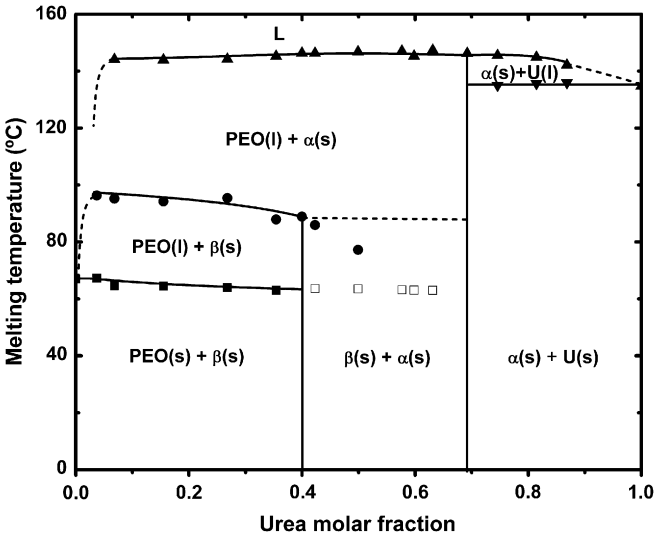

Fig. 8. Phase diagram of PEO–urea binary system. The open symbols represent the melting events due to kinetic products and the dashed lines the expected behavior under thermodynamic conditions.

bonded network between PEO and urea as well as the decreased melting entropy compared with pure urea due to the presence of the polymeric guest. In contrast, the β complex melts incongruently [37] at 89 °C and converts to liquid PEO and α complex. It is interesting to note that the layered complex of PEO with MRES, which was found to be thermodynamically stable, can also melt incongruently to generate the higher melting point complex [22]. The lower melting temperature of the β complex is due to its sandwich structure, in which urea and PEO layers are joined by hydrogen bonds but only van der Waals forces exist within the PEO layers [2]. A liquid phase characterized by significant hydrogen bonding between the urea and PEO is formed above the melting point of the α complex.

The phase separation observed upon melt-cooling the α (Fig. 1) and β (Fig. 4) complexes can be interpreted in view of the new phase diagram. In both cases, crystallization of the stoichiometric complex is slower and/or requires a larger undercooling than that of the next stable urea-rich compound. In the case of the α complex, crystallization of pure urea is kinetically favored and occurs around 90 °C, a temperature at which a "pseudo-tie line" on the phase diagram leads to a second phase with the β complex composition. As predicted from the phase diagram, cooling the melt α complex at a slow rate leads to the direct formation of the thermodynamic product: the solid α complex. In the case of the β complex, the system must first be cooled through a large temperature range, between 143 and 89 °C, where the two equilibrium phases are solid α complex and liquid PEO. It is therefore not surprising that those phases are obtained experimentally (Figs. 4 and 5) in spite of the stability of the complex. The crystallization peak for the α complex is observed at 75 °C in Fig. 4, a temperature below the melting point of the β complex but at which the undercooling is still insufficient for rapid β complex nucleation. Support for this interpretation is obtained by quenching the melt β complex in liquid nitrogen. In such case, the temperature quickly reaches a sufficient undercooling and only the stable β complex is produced.

The phase diagram can further be separated in three main composition ranges. When $X_U > 0.692$, the samples consist of a mixture of solid urea and α complex that sequentially melt at 135 and 143 °C. When $X_U < 0.4$, samples consist of a mixture of PEO with the β complex, in agreement with the conclusion of thermodynamic stability. Otherwise, a tie line would have rather predicted the coexistence of solid PEO and α complex. While a fraction of the PEO chains certainly exist in the amorphous state, its crystallinity level is high and a glass transition temperature is hardly observed except for the pure polymer. Finally, samples with $0.4 > X_U > 0.692$ should in principle be composed of a mixture of the two solid complexes, but a weak PEO melting event is systematically observed, as noted with open squares in Fig. 8. This is explained by the relative crystallization kinetics for the different species. It was shown above that the α complex crystallization is much faster than that of the β complex. As a consequence, more α crystals are formed during the rapid electrospinning process than would be expected under equilibrium conditions. Since the α complex contains more urea than the β complex, this excess crystallization leads to residual pure PEO in the system. When composition is very close to $X_U = 0.692$, the α complex formation is so efficient that almost all urea becomes included in it and the sample consists of a mixture of α complex with a small amount of PEO and only traces of the β complex. We believe that the equilibrium phase diagram should not feature this PEO melting event but rather the β complex melting at a constant temperature marked by the dashed line, but preparing equilibrium samples has proven difficult.

It is interesting to point out that the observation of the stability of the β complex could open up an intriguing new avenue for electrospinning. While the method is normally used to prepare nanofibers of various polymers and complex polymeric systems, it has also been used to prepare unusual or metastable crystal structure [29,30]. This was actually a rationale for using it in the first place to prepare pure β complex samples. The results obtained here demonstrate that electrospinning can also be used to prepare thermodynamically stable compounds that would otherwise be inaccessible under normal sample preparation conditions because of the formation of kinetically frozen products. The method does not require thermal annealing of the as-prepared electrospun fibers. This is especially the case for compounds that melt incongruently and are therefore prone to phase separation upon cooling or solvent evaporation at slower rates than that occurring during an electrospinning experiment.

4. Conclusions

This study has revisited the poly(ethylene oxide)–urea system to better understand the thermodynamic stability and phase behavior of its two molecular complexes. It was demonstrated that the β complex is stable when it is pure, in contrast with the metastable mixture of β complex and urea obtained by melt-quenching the α complex. It was found that the kinetic solid–solid β–α phase transition of such melt-quenched sample occurs over a much longer time scale than previously reported, with a fast local scale reorganization occurring in a few minutes at 60 °C but completion of the inclusion complex formation requiring days. Melt-cooling the pure β complex can also lead to a phase-separated mixture of PEO and α complex due to slower crystallization kinetics. A complete phase diagram was obtained from DSC, WAXD and FT-IR studies and was used to understand the many phases that can coexist under various sample preparation conditions. These results help us to better understand the properties of the important class materials that are polymeric host–guest systems, in particular in view of their application as electrospun nanofibers. More generally, this work also demonstrates that electrospinning is not only a method of choice to prepare metastable structures, but that it can also be used to gain access to stable systems that are otherwise inaccessible due to kinetic freezing. We are currently extending this approach to the preparation of other polymeric host–guest systems.

Acknowledgements

The financial support of the Natural Sciences and Engineering Research Council of Canada (NSERC) and the Fonds Québécois de Recherche sur la Nature et les Technologies (FQRNT) is acknowledged.

References

[1] Liu Y, Pellerin C. Macromolecules 2006;39(26):8886–8.
[2] Liu Y, Antaya H, Pellerin C. Journal of Polymer Science, Part B: Polymer Physics 2008;46(18):1903–13.
[3] Tadokoro H, Yoshihara T, Chatani Y, Murahashi S. Journal of Polymer Science, Part B: Polymer Physics 1964;2:363–8.
[4] Chenite A, Brisse F. Macromolecules 1991;24(9):2221–5.
[5] Vasanthan N, Shin ID, Tonelli AE. Macromolecules 1996;29(1):263–7.
[6] Wagner J-F, Dosière M, Guenet J-M. Macromolecular Symposia 2005;222:121–4.
[7] Suehiro K, Nagano Y. Macromolecular Chemistry and Physics 1983;184(5):669–74.
[8] Bogdanov B, Michailov M, Uzov C, Gavrailova G. Macromolecular Chemistry and Physics 1994;195(6):2227–31.
[9] Bogdanov B, Mikhailov M, Uzov K, Gavrailova G. Die Angewandte Makromolekulare Chemie 1992;195(1):165–70.
[10] Bogdanov B, Mikhailov M, Uzov K, Gavrailova G. Journal of Polymer Science, Part B: Polymer Physics 1994;32(2):387–94.
[11] Bogdanov B, Uzov C, Gavrailova G. Acta Polymerica 1994;45(5):381–4.
[12] Choi C, Davis DD, Tonelli AE. Macromolecules 1993;26(6):1468–70.
[13] Vasanthan N, Shin ID, Tonelli AE. Macromolecules 1994;27(22):6515–9.
[14] Howe C, Vasanthan N, MacClamrock C, Sankar S, Shin ID, Simonsen IK, et al. Macromolecules 1994;27(25):7433–6.
[15] Hollingsworth MD, Harris KDM. In: Atwood JL, Davies JED, MacNicol DD, Vogtle F, editors. Comprehensive supramolecular chemistry, vol. 6. Oxford: Elsevier Science Ltd.; 1996. p. 177–237.
[16] Ye HM, Peng M, Xu J, Guo BH, Chen Q, Yun TL, et al. Polymer 2007;48(25):7364–73.
[17] Delaite E, Point JJ, Damman P, Dosière M. Macromolecules 1992;25(18):4768–78.
[18] Damman P, Point JJ. Macromolecules 1993;26(7):1722–8.
[19] Damman P, Point JJ. Macromolecules 1994;27(14):3919–25.
[20] Damman P, Point JJ. Macromolecules 1995;28(6):2050–3.
[21] Spevacek J, Paternostre L, Damman P, Draye AC, Dosière M. Macromolecules 1998;31(11):3612–6.
[22] Paternostre L, Damman P, Dosière M. Macromolecules 1999;32(1):153–61.
[23] Iannelli P, Damman P, Dosière M, Moulin J-F. Macromolecules 1999;32(7):2293–300.
[24] Greiner A, Wendorff JH. Angewandte Chemie International Edition 2007;46(30):5670–703.
[25] Yarin AL, Koombhongse S, Reneker DH. Journal of Applied Physics 2001;89(5):3018–62.
[26] Burger C, Hsiao BS, Chu B. Annual Review Materials Research 2006;36:333–68.
[27] Kakade MV, Givens S, Gardner K, Lee KH, Chase DB, Rabolt JF. Journal of the American Chemical Society 2007;129(10):2777–82.
[28] Kongkhlang T, Tashiro K, Kotaki M, Chirachanchai S. Journal of the American Chemical Society 2008;130(46):15460–6.
[29] Stephens JS, Chase DB, Rabolt JF. Macromolecules 2004;37(3):877–81.
[30] Lee K-H, Snively CM, Givens S, Chase DB, Rabolt JF. Macromolecules 2007;40(7):2590–5.
[31] Gowd EB, Shibayama N, Tashiro K. Macromolecules 2007;40(17):6291–5.
[32] Gowd EB, Shibayama N, Tashiro K. Macromolecules 2008;41(7):2541–7.
[33] Vaughan P, Donohue J. Acta Crystallographica 1952;5(6):530–5.
[34] Zavodnik V, Stash A, Tsirelson R, Vries R, Feil D. Acta Crystallographica Section B 1999;B55(1):45–54.
[35] Zhang H, Xuan X, Wang J, Wang H. Journal of Physical Chemistry B 2004;108(5):1563–9.
[36] Brandrup J, Immergut EH, Grulke EA, editors. Polymer handbook. 4th ed. Hoboken: John Wiley & Sons; 1999 [chapter VI].
[37] White MA, Harnish RS. Chemistry of Materials 1998;10(3):833–9.